Using an Autonomous Underwater Vehicle to Track a Coastal Upwelling Front

Yanwu Zhang, *Senior Member, IEEE*, Michael A. Godin, James G. Bellingham, *Member, IEEE*, and John P. Ryan

***Abstract*—Coastal upwelling is a wind-driven ocean process. It brings cooler, saltier, and usually nutrient-rich deep water upward to replace surface water displaced offshore due to Ekman transport. The nutrients carried up by upwelling are important for primary production and fisheries. Ocean life can aggregate at the boundary between stratified water and upwelling water—the upwelling front. In an upwelling water column, temperature, salinity, and other water properties are much more homogeneous over depth than in stratified water. Drawing on this difference, we set up a key measure for differentiating upwelling and stratified water columns—the vertical temperature difference between shallow and deep depths. The vertical temperature difference is large in stratified water but small in upwelling water. Based on this classifier, we developed a method for an autonomous underwater vehicle (AUV) to autonomously detect and track an upwelling front. During the Controlled, Agile, and Novel Observing Network (CANON) Experiment in April 2011, the Tethys long-range AUV ran the algorithm to autonomously track an upwelling front in a dynamic coastal upwelling region in Monterey Bay, CA. The AUV transected the upwelling front 14 times over two days, providing a very high-resolution depiction of the front.**

***Index Terms*—Autonomous underwater vehicle (AUV), upwelling front, tracking.**

I. Introduction

An ocean front delineates the boundary between water masses distinguished by different physical, chemical, and/or biological characteristics. Ocean ecosystems are greatly influenced by the structure and dynamics of fronts [1]. Ocean fronts also play an important role in air–sea exchange [2], [3]. Detection and tracking of ocean fronts are important for investigating the formation, evolution, and interaction of ocean water masses. Knowing the boundary between these water masses enables targeted sampling of the respective waters.

As surface water is warmed by sunlight, temperature at surface is higher than at depth, so density increases with depth, forming a stratified water column that is gravitationally stable [4]. Coastal upwelling [5], as illustrated in Fig. 1, is a wind-driven ocean process that breaks stratification thus making water more homogeneous over depth. Suppose a northerly (i.e., from the north) wind blows along a north–south coastline in the northern hemisphere. The wind stress plus the effect of Earth's rotation will lead to a net transport of surface water offshore, called Ekman transport [6]. To conserve mass, deep water wells up to replace the displaced surface water. Upwelling brings cooler, saltier, and usually nutrient-rich deep water upward, replacing warmer, fresher, and nutrient-depleted surface water. The nutrients carried up by upwelling have significant impact on primary production and fisheries.

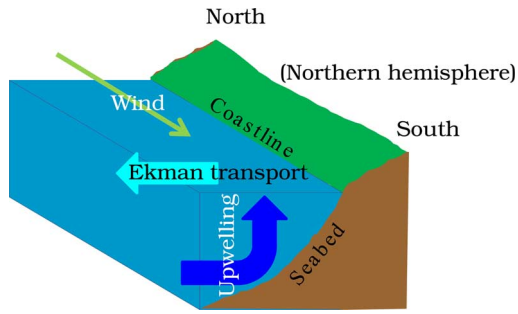

Fig. 1. Illustration of a northerly wind driving upwelling along a north–south coastline in the northern hemisphere.

When a northwesterly wind persists in spring and summer along the California coastline, intense upwelling takes place at Point Año Nuevo (to the northwest of Monterey Bay, CA; see Fig. 2) [7]. For instance, during the April 2011 Controlled, Agile, and Novel Observing Network (CANON) Experiment, upwelling of cold deep water to the surface was manifested by low sea surface temperature (SST) at Point Año Nuevo and in the upwelling filaments spreading southward from Point Año Nuevo, as displayed in Fig. 2. Due to the presence of a mountain range along the northern coast, the northern Monterey Bay is less exposed to the strong northwesterly wind forcing that drives upwelling along the coast. The northern bay is also sheltered from the prevailing southward flow of upwelling filaments (from Point Año Nuevo) by its coastal recess. Such atmospheric and oceanic sheltering, as well as bay circulation patterns, causes enhanced residence time and local heating in the northern bay, a region described as the Monterey Bay "upwelling shadow" [1], [8], [9], manifested by relatively high SST in the northern bay, as displayed in Fig. 2. The boundary between the stratified water in the upwelling shadow and the unstratified water transported southward from the Point Año Nuevo upwelling center is called the "upwelling front." Upwelling fronts support enriched phytoplankton and zooplankton populations [1], [10], thus having great influences on ocean ecosystems. The SST images in Fig. 2 also demonstrate the dynamic evolution of the upwelling front over a two-day period in April 2011. Note that satellite SST only provides the surface expression of upwelling processes. Also, the large data interval (on the order of a day) renders satellite SST data insufficient for providing high-resolution tracking of frontal dynamics.

Manuscript received September 14, 2011; revised March 02, 2012; accepted April 21, 2012. Date of publication June 06, 2012; date of current version July 10, 2012. This work was supported by the David and Lucile Packard Foundation.

Associate Editor: W. M. Carey.

The authors are with the Monterey Bay Aquarium Research Institute, Moss Landing, CA 95039 USA (e-mail: yzhang@mbari.org).

Digital Object Identifier 10.1109/JOE.2012.2197272

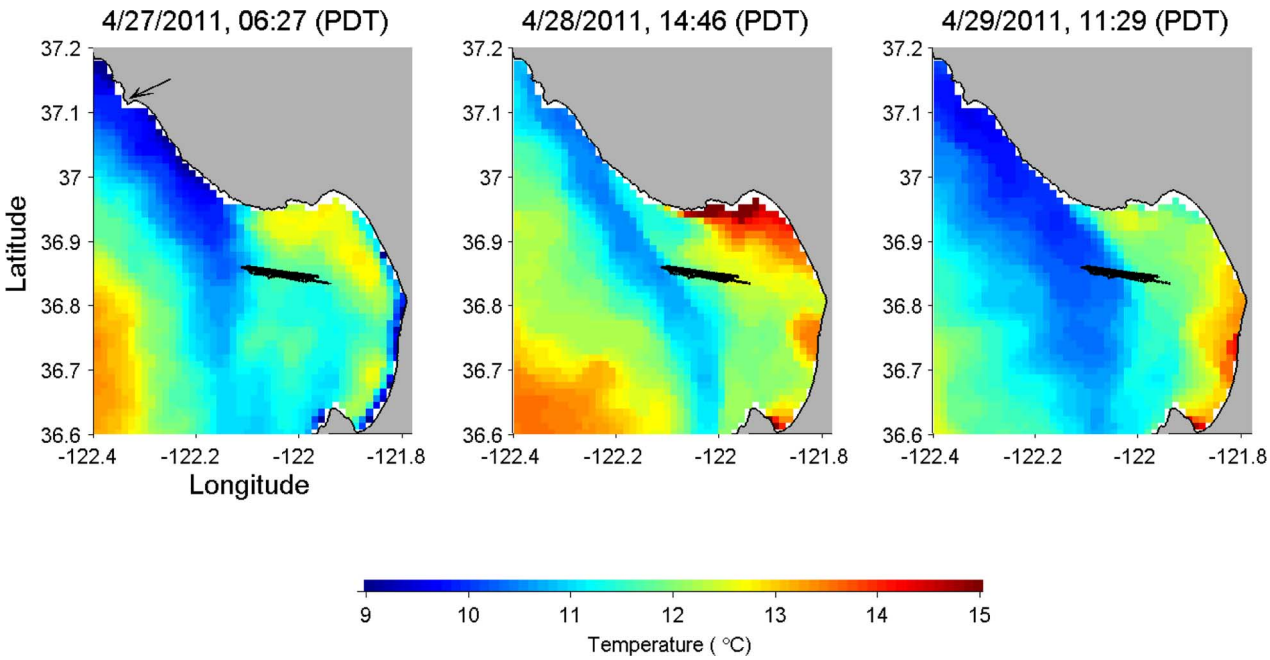

Fig. 2. Sea surface temperature (SST) in Monterey Bay, CA from April 27 to 29 during the April 2011 CANON Experiment. Point Año Nuevo (to the northwest of Monterey Bay) is marked by the black arrow in the left panel. The Tethys AUV's horizontal trajectory in tracking the upwelling front [from April 27 12:12:00 to April 29 15:22:00 (PDT)] is shown by the black lines (see Section III). Advanced Very High Resolution Radiometer (AVHRR) SST data courtesy of Kudela Lab. (University of California at Santa Cruz) and the National Oceanographic and Atmospheric Administration (NOAA) CoastWatch. Longitude: West. Latitude: North.

Autonomous underwater vehicles (AUVs) can be effectively used for studying ocean fronts. In the 1996 Haro Strait Frontal Dynamics Experiment [11], [12], two Massachusetts Institute of Technology (MIT, Cambridge) Odyssey-class AUVs were deployed along with surface ships and drifters in a coordinated effort to map the tidal fronts. The AUVs conducted high-resolution surveys of temperature, salinity, and current velocity in the frontal regions [13], [14]. For frontal mapping by acoustic tomography [11], an acoustic source was also installed on one vehicle. During the experiment, the Harvard Ocean Prediction System (HOPS) ocean model [15] was run to predict the front's location, which guided the AUVs' deployment. However, the AUVs did not possess the ability to autonomously detect the front.

In [16]–[22], AUVs were used to detect and track the thermocline based on the temperature gradient in the vertical dimension. In [23], an autonomous surface craft was used to estimate the direction of the horizontal thermal gradient based on temperature measurements. In [24], an adaptive control capability was demonstrated for enabling three gliders to move in a triangular formation toward a low-temperature region in Monterey Bay.

A prior effort aimed at detection and tracking of fronts in Monterey Bay involved an approach called "mixed initiative" [25]. This approach begins with an AUV conducting a reconnaissance survey and sending a compressed data set back to a scientist onshore via satellite. The scientist examines the data for the presence of a front and derives parameters that will permit the AUV to locate the center of the front: 1) the depth at which to transit during the search; and 2) the water temperature at the center of the front at the search depth. This data-informed human initiative is relayed back to the AUV and thereafter integrated with machine initiative for the AUV to track the front using a repeated sequence of localization and mapping. These capabilities successfully demonstrated adaptive control of an AUV using onboard planning and execution. However, the requirement for a human in the loop imposes limitations.

We have developed two different methods for an AUV to autonomously detect and track an upwelling front. One method is for an AUV to detect and accurately locate an upwelling front based on the horizontal gradient of the vertical temperature difference between shallow and deep depths [26]. The algorithm was successfully run on the Dorado AUV for triggering water samplings within a narrow upwelling front in Monterey Bay, during the June 2011 CANON Experiment. Another method, initially reported in [27] and fully presented in this paper, is for an AUV to recognize that it has departed from a stratified water column and entered an upwelling water column (or conversely), and accordingly track the front between the two distinct water columns. The AUV distinguishes between the two types of water columns based on their distinction in vertical homogeneity of temperature. The algorithm is presented in Section II. In the April 2011 CANON Experiment, the Tethys AUV [28] ran our algorithm to track an upwelling front in Monterey Bay, as described in Section III. We propose future work in Section IV.

II. An AUV Algorithm for Tracking an Upwelling Front

The different vertical temperature structures in stratified and upwelling water columns, and in the narrow front between them, are illustrated in Fig. 3. The key to classification is finding the

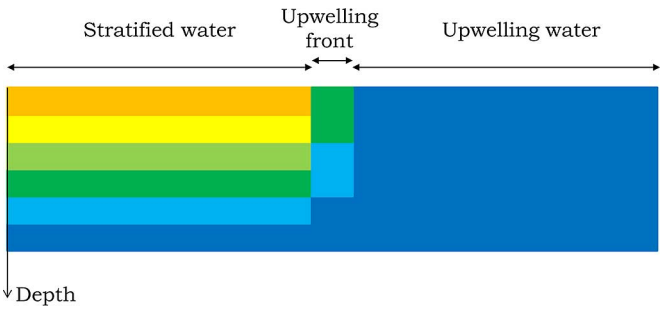

Fig. 3. Illustration of different vertical temperature structures in stratified and upwelling water columns, and in the narrow front between them. Temperature from high to low is represented by color ranging from orange to blue (i.e., the temperature decreases with depth).

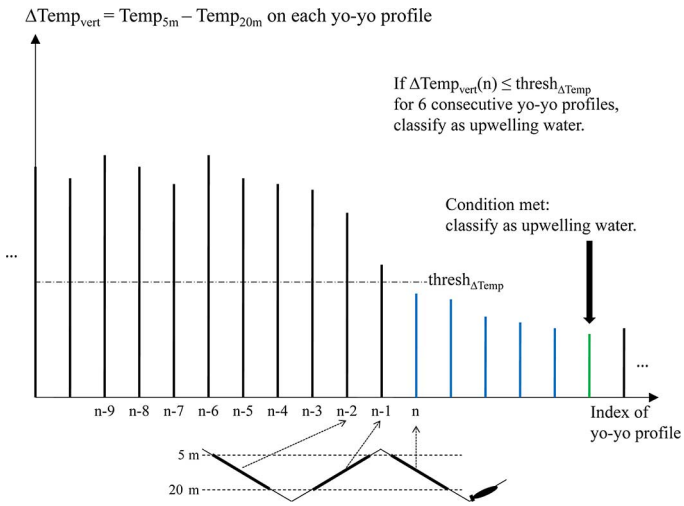

Fig. 4. Illustration of the algorithm for an AUV to determine that it has departed from a stratified water column and entered an upwelling water column. The first five yo–yo profiles that satisfy $\Delta\mathrm{Temp}_{\mathrm{vert}} \leq \mathrm{thresh}_{\Delta\mathrm{Temp}}$ but $\mathrm{Count}_{\mathrm{FrontDetected}} < 6$ are marked blue. The sixth yo–yo profile that satisfies $\Delta\mathrm{Temp}_{\mathrm{vert}} \leq \mathrm{thresh}_{\Delta\mathrm{Temp}}$ and $\mathrm{Count}_{\mathrm{FrontDetected}} = 6$ is marked green.

feature that maximizes the separability between classes. In the upwelling water column, the vertical temperature difference between shallow and deep depths is small due to the upwelling process; but in the stratified water column, the vertical temperature difference is large (warm at surface and cold at depth). Drawing on this difference, we set up a key measure for differentiating upwelling and stratified water columns—the vertical temperature difference in the water column [27]

$$\Delta\mathrm{Temp}_{\mathrm{vert}} = |\mathrm{Temp}_{\mathrm{shallow}} - \mathrm{Temp}_{\mathrm{deep}}| \tag{1}$$

where $\mathrm{Temp}_{\mathrm{shallow}}$ and $\mathrm{Temp}_{\mathrm{deep}}$ are temperatures at shallow and deep depths, respectively. $\Delta\mathrm{Temp}_{\mathrm{vert}}$ is significantly smaller in upwelling water than in stratified water.

If $\Delta\mathrm{Temp}_{\mathrm{vert}}$ falls below a threshold $\mathrm{thresh}_{\Delta\mathrm{Temp}}$, the water column is classified as an upwelling water column

$$\Delta\mathrm{Temp}_{\mathrm{vert}}(n) \leq \mathrm{thresh}_{\Delta\mathrm{Temp}}. \tag{2}$$

Suppose an AUV flies from stratified water to upwelling water on a sawtooth (i.e., yo–yo) trajectory (in the vertical dimension). The algorithm for the AUV to determine that it has departed from the stratified water column and entered the upwelling water column is illustrated in Fig. 4. Previous temperature measurements in Monterey Bay indicated that $\Delta\mathrm{Temp}_{\mathrm{vert}}$ between 5- and 20-m depths provided a strong contrast between upwelling and stratified water columns. Hence, we set the shallow depth to 5 m and the deep depth to 20 m in (1). For classification, we set the threshold $\mathrm{thresh}_{\Delta\mathrm{Temp}} = 1°C$ (again based on previous AUV temperature measurements in Monterey Bay) in (2).

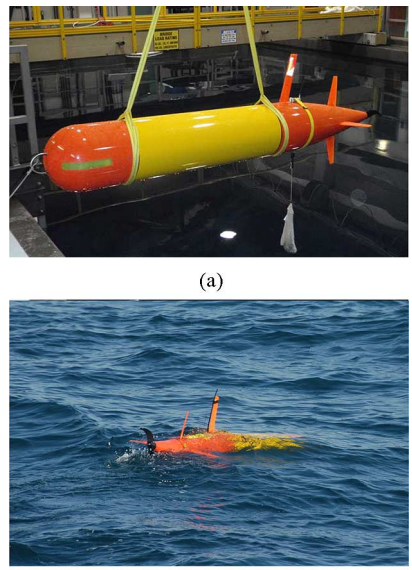

(a)

(b)

Fig. 5. The Tethys AUV (a) suspended over MBARI's test tank and (b) deployed in Monterey Bay. The orange tail section of the vehicle is the propulsion and control section, which also includes antennas for Iridium and Argos satellites, GPS, and line-of-sight radio-frequency communications. The yellow center section is the main pressure vessel housing vehicle electronics and batteries. The orange head section is a wet volume housing a suite of science sensors.

On each yo–yo profile (descent or ascent), the AUV records $\mathrm{Temp}_{5\,\mathrm{m}}$ and $\mathrm{Temp}_{20\,\mathrm{m}}$ to calculate $\Delta\mathrm{Temp}_{\mathrm{vert}} = |\mathrm{Temp}_{5\,\mathrm{m}} - \mathrm{Temp}_{20\,\mathrm{m}}|$. When $\Delta\mathrm{Temp}_{\mathrm{vert}}$ falls below $\mathrm{thresh}_{\Delta\mathrm{Temp}}$ for six consecutive yo–yo profiles, the AUV determines that it has entered an upwelling water column. The requirement of $\Delta\mathrm{Temp}_{\mathrm{vert}}$ on six consecutive yo–yo profiles falling below $\mathrm{thresh}_{\Delta\mathrm{Temp}}$ is for robust detection of an upwelling water column (i.e., small patches of water with low $\Delta\mathrm{Temp}_{\mathrm{vert}}$ will be ignored).

Conversely, suppose an AUV flies from upwelling water to stratified water on a yo–yo trajectory (in the vertical dimension). When $\Delta\mathrm{Temp}_{\mathrm{vert}}$ rises above $\mathrm{thresh}_{\Delta\mathrm{Temp}}$ for six consecutive yo–yo profiles, the AUV determines that it has entered a stratified water column. The requirement of $\Delta\mathrm{Temp}_{\mathrm{vert}}$ on six consecutive yo–yo profiles rising above $\mathrm{thresh}_{\Delta\mathrm{Temp}}$ is for robust detection of a stratified water column (i.e., small patches of water with high $\Delta\mathrm{Temp}_{\mathrm{vert}}$ will be ignored).

Based on the above classification algorithm, we developed a method for an AUV to track the upwelling front as follows [27].

- Suppose an AUV starts a mission in stratified water and flies toward upwelling water on a yo–yo trajectory (in the vertical dimension). When $\Delta\mathrm{Temp}_{\mathrm{vert}}$ falls below $\mathrm{thresh}_{\Delta\mathrm{Temp}}$, a detection counter $\mathrm{Count}_{\mathrm{FrontDetected}}$ counts 1. On the following yo–yo profile, if $\Delta\mathrm{Temp}_{\mathrm{vert}}$

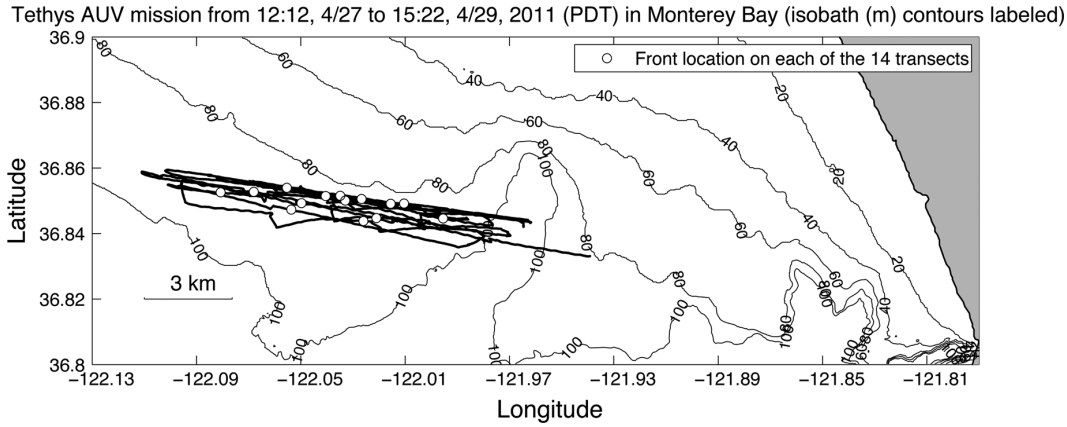

Fig. 6. The horizontal track of the Tethys AUV on April 27–29, 2011 (mission log number 20110427T191236). The AUV transected the front (back and forth) 14 times. The front's location detected on each transect is marked by a white dot (delay corrected).

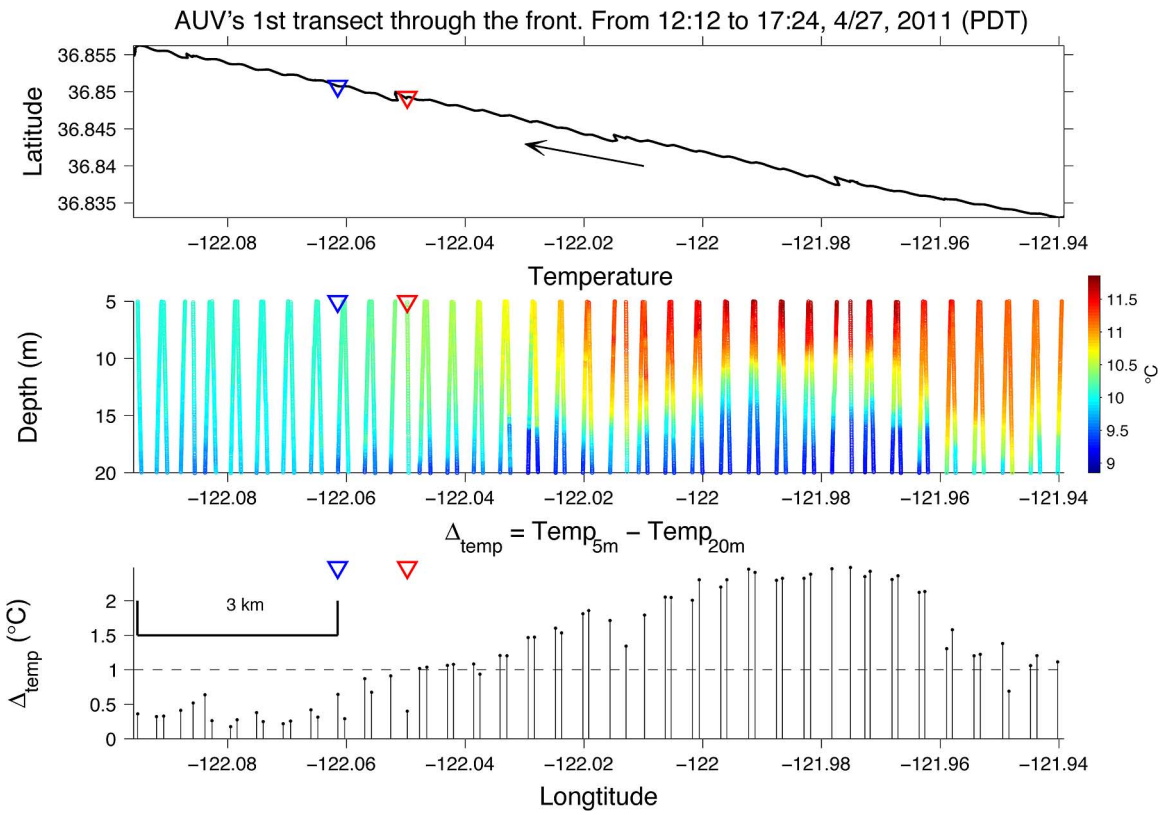

Fig. 7. (a) The horizontal track of the AUV's first transect from stratified water to upwelling water. (b) AUV-measured temperature between 5- and 20-m depths. (c) $\Delta\mathrm{Temp}_{\mathrm{vert}} = \mathrm{Temp}_{5\,m} - \mathrm{Temp}_{20\,m}$ used as the classifier for distinguishing between stratified and upwelling water columns. In each panel, the blue triangle marks the front detection location where the AUV determined that it had passed the front and entered the upwelling water column (i.e., when $\mathrm{Count}_{\mathrm{FrontDetected}}$ reached 6 and hence $\mathrm{Flag}_{\mathrm{PassedFront}}$ was to 1); the red triangle marks the true location of the front (i.e., when $\mathrm{Count}_{\mathrm{FrontDetected}}$ reached 1 prior to reaching 6).

remains below $\mathrm{thresh}_{\Delta\mathrm{Temp}}$, $\mathrm{Count}_{\mathrm{FrontDetected}}$ increases to 2; but if $\Delta\mathrm{Temp}_{\mathrm{vert}}$ turns out to be above $\mathrm{thresh}_{\Delta\mathrm{Temp}}$, $\mathrm{Count}_{\mathrm{FrontDetected}}$ is reset to 0. When $\mathrm{Count}_{\mathrm{FrontDetected}}$ reaches 6, the AUV determines that it has passed the front and entered an upwelling water column, and accordingly sets $\mathrm{Flag}_{\mathrm{PassedFront}}$ to 1.

- The AUV continues flight in the upwelling water for $\mathrm{Dist}_{\mathrm{continuation}} = 3$ km to sufficiently cover the frontal region, and then turns around to fly back to the stratified water. $\mathrm{Count}_{\mathrm{FrontDetected}}$ and $\mathrm{Flag}_{\mathrm{PassedFront}}$ are reset to 0.
- On the way back to the stratified water, when $\Delta\mathrm{Temp}_{\mathrm{vert}}$ rises above $\mathrm{thresh}_{\Delta\mathrm{Temp}}$, $\mathrm{Count}_{\mathrm{FrontDetected}}$ counts 1. When $\mathrm{Count}_{\mathrm{FrontDetected}}$ reaches 6, the AUV determines that it has passed the front and entered the stratified water column, and accordingly sets $\mathrm{Flag}_{\mathrm{PassedFront}}$ to 1.
- The AUV continues flight in the stratified water for $\mathrm{Dist}_{\mathrm{continuation}} = 3$ km, and then turns around to fly back to the upwelling water. $\mathrm{Count}_{\mathrm{FrontDetected}}$ and $\mathrm{Flag}_{\mathrm{PassedFront}}$ are reset to 0.
- The AUV repeats the above cycle of front crossing. As the front evolves over time, the AUV effectively tracks it.

III. Field Performance

The Tethys long-range AUV [28], as shown in Fig. 5, was developed at the Monterey Bay Aquarium Research Institute

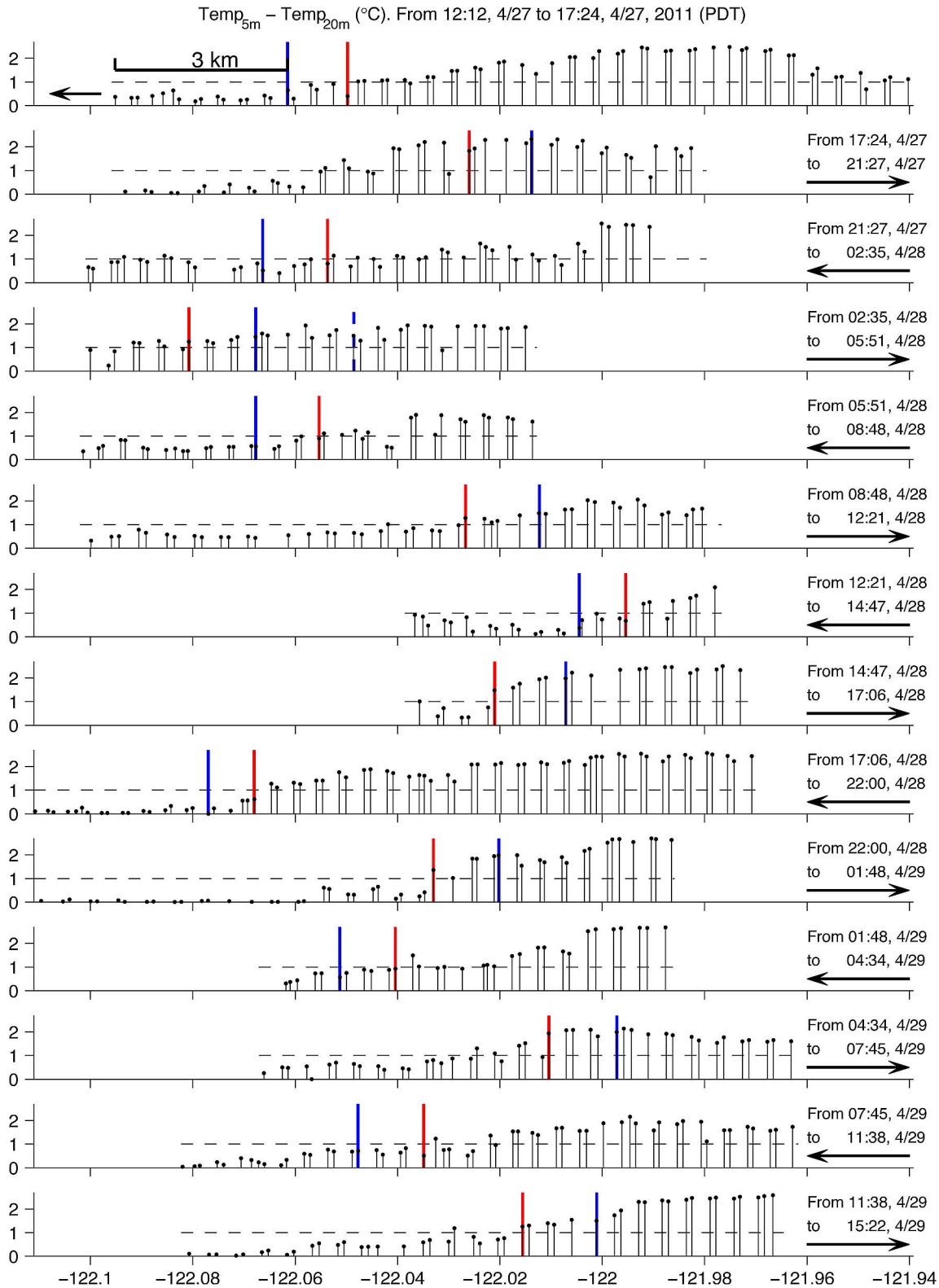

Fig. 8. $\Delta\mathrm{Temp}_{\mathrm{vert}} = \mathrm{Temp}_{5\,\mathrm{m}} - \mathrm{Temp}_{20\,\mathrm{m}}$ on all the 14 transects. The AUV's flight direction on each transect is shown by the arrow. The blue vertical bar marks the front detection location (i.e., when $\mathrm{Count}_{\mathrm{FrontDetected}}$ reached 6 and hence $\mathrm{Flag}_{\mathrm{PassedFront}}$ was set to 1); the red vertical bar marks the true location of the front (i.e., when $\mathrm{Count}_{\mathrm{FrontDetected}}$ reached 1 before reaching 6). The duration of each transect is also noted.

(MBARI). It has a length of 2.3 m and a diameter of 0.3 m (i.e., 12 in) at the midsection. The propeller-driven vehicle can run effectively from 0.5 to 1 m/s. Propulsion power consumption is minimized through a careful design of a low-drag body and a high-efficiency propulsion system. In addition, by using a buoyancy engine, the vehicle is capable of trimming to neutral buoyancy and drifting in a lower power mode. The Tethys AUV thus combines the merits of propeller-driven and buoyancy-driven vehicles. The vehicle's sensor suite includes Neil Brown temperature and conductivity sensors, a Keller depth

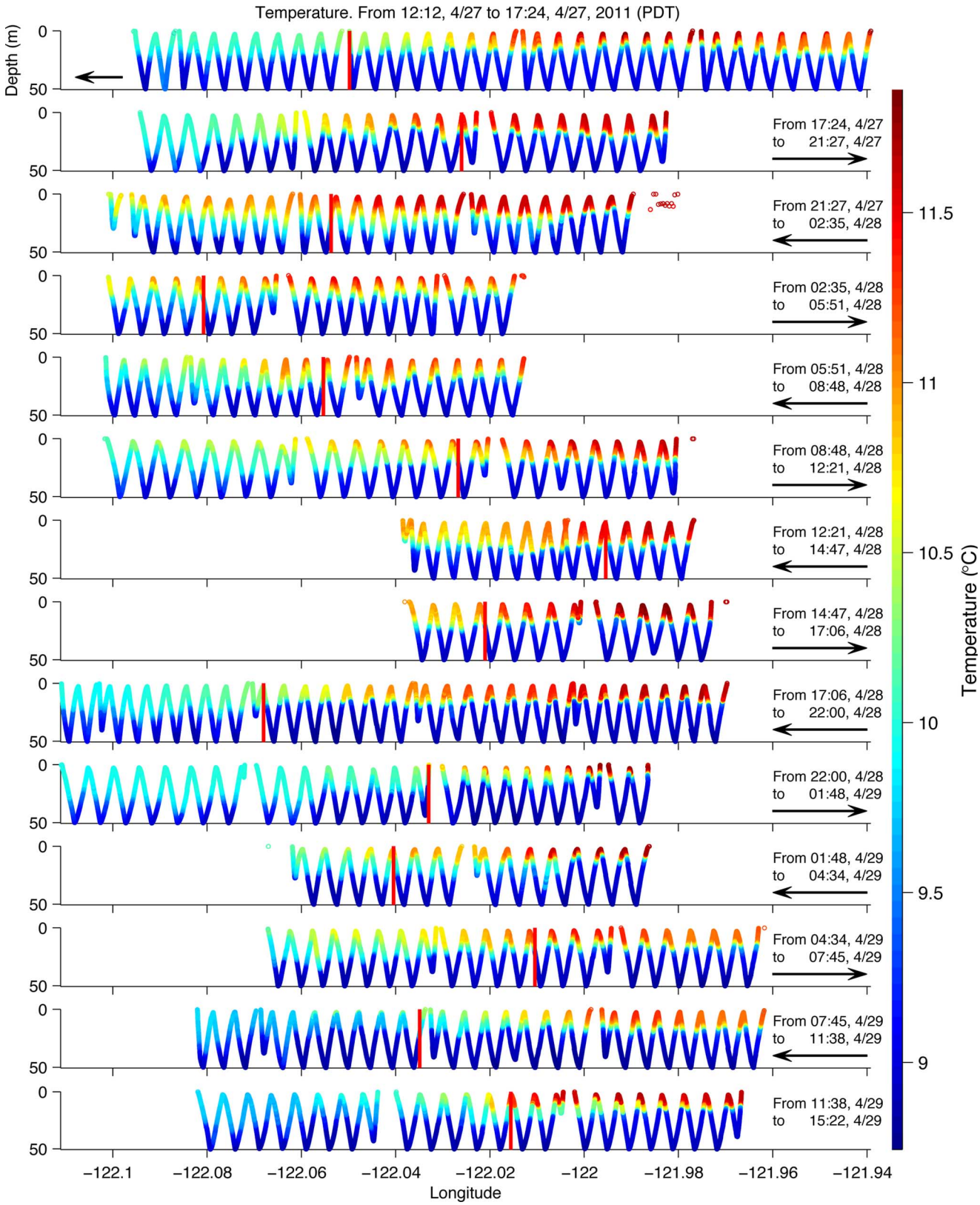

Fig. 9. AUV-measured temperature from surface to the full AUV depth of 50 m. On each transect, the red vertical bar marks the true (i.e., delay-corrected) location of the front.

sensor, a WET Labs ECO-Triplet Puck fluorescence/backscatter sensor, an Aanderaa dissolved oxygen sensor, an In Situ Ultraviolet Spectrophotometer (ISUS) nitrate sensor, and a LinkQuest Doppler velocity log (DVL) of Model NavQuest 600 Micro.

The AUV's underwater navigation is by DVL-aided dead reckoning. The DVL provides the Earth-referenced velocity of the AUV when the ocean bottom is within range (110 m). The vehicle's estimated speed is combined with measured heading

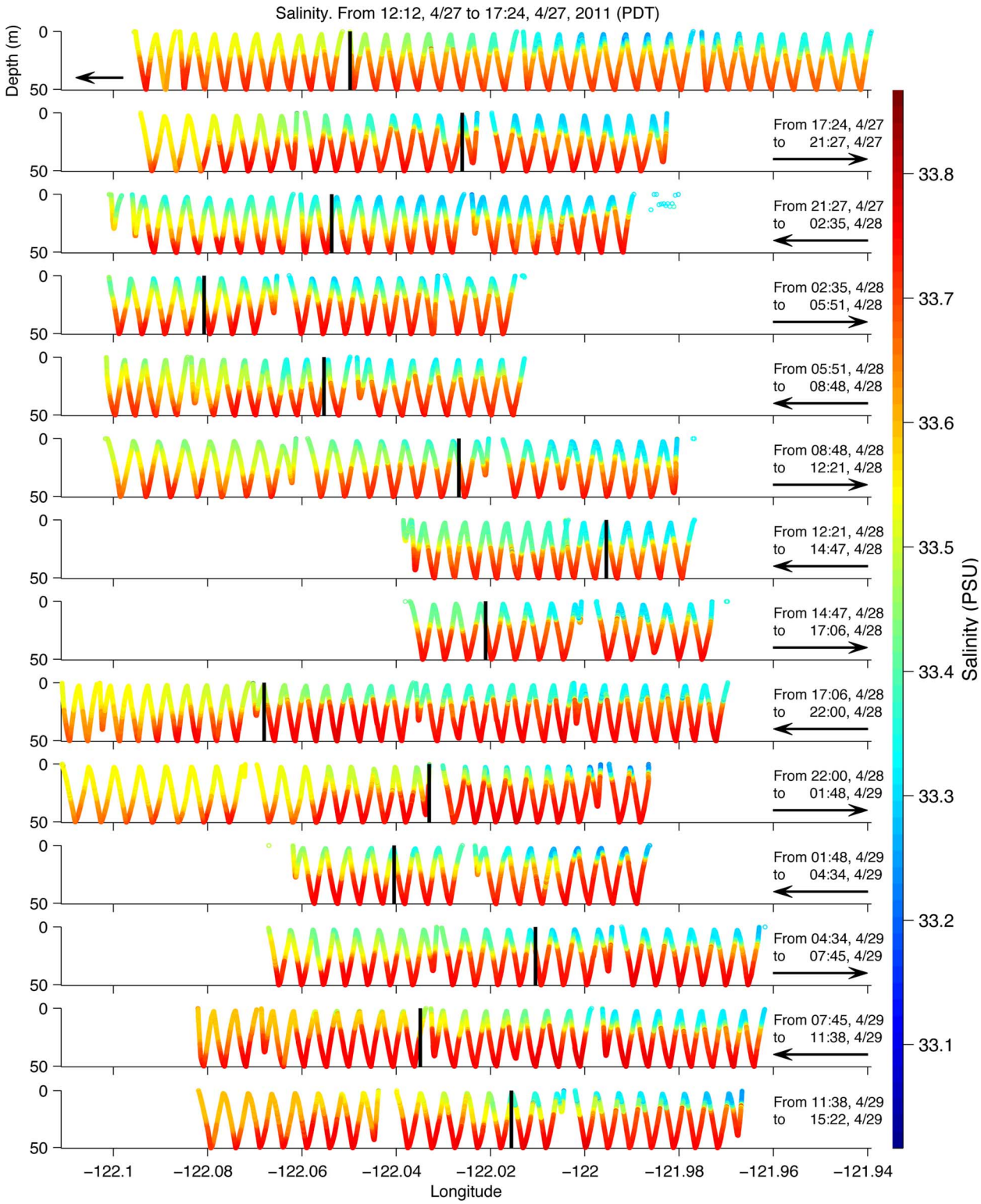

Fig. 10. AUV-measured salinity from surface to the full AUV depth of 50 m. On each transect, the black vertical bar marks the true (i.e., delay-corrected) location of the front.

and attitude and then accumulated to provide the estimated location of the AUV. The vehicle periodically ascends to the surface for a Global Positioning System (GPS) fix to correct the AUV's underwater navigation error [29].

One of the science objectives of the April 2011 CANON Experiment was to study the dynamics of upwelling fronts in Monterey Bay. From April 27 to 29, the Tethys AUV ran the presented algorithm to detect and track an upwelling front (mission log number 20110427T191236). The vehicle's horizontal track is overlaid on Monterey Bay SST images in Fig. 2. The front between the upwelling filament (spreading southward from the Point Año Nuevo upwelling center) and the upwelling shadow water (in the northern bay) is clearly shown by the contrast in SST. The SST images also show the dynamic evolution of the

front over the two-day duration of the AUV mission. However, satellite SST only provided the surface expression of the upwelling process. Also, the large data interval (on the order of a day) rendered the satellite SST data insufficient for providing high-resolution tracking of frontal dynamics.

We deployed the Tethys AUV to fulfill the task of high-resolution front tracking. The AUV flew on a yo–yo trajectory between surface and 50-m depth. A closeup view of the vehicle's horizontal track is displayed in Fig. 6. The AUV's vertical trajectories are shown in Fig. 9. The AUV's average horizontal speed was about 0.87 m/s. Its average vertical speed was 0.23 m/s on ascent or descent legs. Thus, the flight-path angle of the yo–yo trajectory (the angle between the trajectory and the horizontal) was $\beta_{\text{flight\_path}} = \text{atan}\ (0.23/0.87) = 15°$. The vehicle transected the front (back and forth) 14 times over two days, providing a very high-resolution depiction of the frontal dynamics.

As presented in Section II, the AUV used $\Delta\text{Temp}_{\text{vert}} = \text{Temp}_{5\,\text{m}} - \text{Temp}_{20\,\text{m}}$ as the classifier for distinguishing between stratified and upwelling water columns. A detailed view of the first transect through the front is shown in Fig. 7. The AUV started from stratified water, where $\Delta\text{Temp}_{\text{vert}}$ was large. As the vehicle flew toward the upwelling water, $\Delta\text{Temp}_{\text{vert}}$ decreased. When $\Delta\text{Temp}_{\text{vert}}$ fell below $\text{thresh}_{\Delta\text{Temp}} = 1$ °C, $\text{Count}_{\text{FrontDetected}}$ began to count. When $\text{Count}_{\text{FrontDetected}}$ reached 6, the AUV determined that it had passed the front and entered the upwelling water, and accordingly set $\text{Flag}_{\text{PassedFront}}$ to 1 (i.e., the front was detected), as marked by the blue triangle. Thus, the AUV's detection of the front came with a delay due to the requirement $\text{Count}_{\text{FrontDetected}} = 6$. The true location of the front was when $\text{Count}_{\text{FrontDetected}}$ reached 1 prior to reaching 6, as marked by the red triangle. The AUV continued flight into the upwelling water for $\text{Dist}_{\text{continuation}} = 3$ km to sufficiently cover the frontal region.

$\Delta\text{Temp}_{\text{vert}}$ on all the 14 transects is shown in Fig. 8. For each transect, the AUV's flight direction is shown by the arrow, and the duration is also noted. On each transect, the blue vertical bar marks the front detection location (i.e., when $\text{Count}_{\text{FrontDetected}}$ reached 6); the red vertical bar marks the true location of the front (i.e., when $\text{Count}_{\text{FrontDetected}}$ reached 1 prior to reaching 6). After detection of the front, the AUV continued flight for 3 km to sufficiently cover the frontal region. Additional explanations of the fourth and eleventh transects are as follows. On the fourth transect, near longitude 122.07° W, the AUV detected the front (i.e., when $\text{Count}_{\text{FrontDetected}}$ reached 6 and hence $\text{Flag}_{\text{PassedFront}}$ was set to 1), as marked by the blue solid vertical bar (the true location of the front is marked by the red solid vertical bar). Just after that, the experimental code run on the AUV caused a timing error in the communication between the main computer and the propeller's motor controller, which resulted in an early termination of the mission. Then, the shore operator restarted the AUV mission ($\text{Count}_{\text{FrontDetected}}$ and $\text{Flag}_{\text{PassedFront}}$ were reset to 0), maintaining the flight direction into the stratified water. When $\text{Count}_{\text{FrontDetected}}$ reached 6 again, $\text{Flag}_{\text{PassedFront}}$ was set to 1 again, which is marked by the blue dashed vertical bar. This second detection actually occurred inside the stratified water and should be ignored. On the eleventh transect, the aforementioned experimental code caused another communication error which resulted in an early termination of the mission. Then, the shore operator restarted the AUV mission on the reverse direction (i.e., the ensuing twelfth transect). The code causing the communication errors was corrected after the experiment.

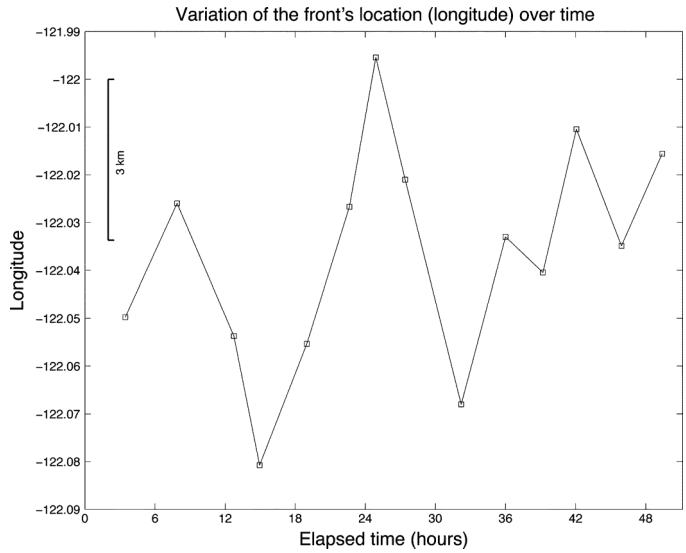

Fig. 11. Temporal variation of the front's location (marked by the small squares which correspond to the red vertical bars in Fig. 9) on the 14 transects over two days.

The AUV-measured temperature and salinity from surface to the full AUV depth of 50 m on all the 14 transects are shown in Figs. 9 and 10, respectively. In the upwelling water (to the west of the front), temperature and salinity were both much more homogeneous over depth than in the stratified water (to the east of the front). Also, in the upwelling water, temperature was lower and salinity was higher than in the stratified water, consistent with the expected properties of upwelling water.

The front's locations detected on the 14 transects are plotted as a function of time in Fig. 11. On average, the AUV crossed the front every 3.5 h, thus closely tracking the front for two days. The front's location changed from one transect to the next. This variation is due to changes in the direction and intensity of wind (the driving force of upwelling) as well as motions of and interactions between stratified and upwelling water masses.

IV. Conclusion and Discussion

We have developed a method for an AUV to autonomously detect and track an upwelling front. In a two-day mission in April 2011, the Tethys AUV ran the algorithm to closely track an upwelling front in Monterey Bay. The 14 transects across the front provided high-resolution pictures of temperature, salinity, and other water properties (not shown due to space limitation).

In the current algorithm, after the AUV has passed the front (i.e., $\text{Flag}_{\text{PassedFront}}$ is set to 1), the vehicle continues to fly for a preset distance $\text{Dist}_{\text{continuation}}$ before turning around. The purpose of the continued flight is for sufficient coverage of the frontal region. Instead of presetting $\text{Dist}_{\text{continuation}}$, we can let the AUV adjust this parameter based on real-time calculation of the horizontal variability of $\Delta\text{Temp}_{\text{vert}}$. When the horizontal variability of $\Delta\text{Temp}_{\text{vert}}$ remains high, it signifies that the vehicle is still flying in the transitional region (i.e., the frontal re-

gion), so the AUV should continue flight maintaining the direction. When the horizontal variability of $\Delta\mathrm{Temp}_{\mathrm{vert}}$ drops below some level, it signifies that the vehicle has exited the frontal region and entered the upwelling or stratified water column, so the AUV should turn around. This way, the AUV can adaptively strike a good balance between frontal coverage and temporal resolution of front tracking.

ACKNOWLEDGMENT

The authors would like to thank T. Hoover, B. Kieft, B. Hobson, R. McEwen, and D. Klimov for helping with the planning and operation of the Tethys AUV missions. They would also like to thank Dr. F. Chavez and Dr. C. Scholin for their support during the CANON experiments, and R. Kudela and C. Ruhsam (University of California at Santa Cruz) for processing and providing the satellite AVHRR SST data. The authors would also like to thank the anonymous reviewers for their comments and suggestions for improving the paper.

REFERENCES

[1] J. P. Ryan, A. M. Fischer, R. M. Kudela, M. A. McManus, J. S. Myers, J. D. Paduan, C. M. Ruhsam, C. B. Woodson, and Y. Zhang, "Recurrent frontal slicks of a coastal ocean upwelling shadow," *J. Geophys. Res.*, vol. 115, 2010, C12070.

[2] E. D'Asaro, C. Lee, L. Rainville, R. Harcourt, and L. Thomas, "Enhanced turbulence and energy dissipation at ocean fronts," *Science*, vol. 332, no. 6027, pp. 318–322, 2011.

[3] R. Ferrari, "A frontal challenge for climate models," *Science*, vol. 332, no. 6027, pp. 316–317, 2011.

[4] J. Wright, *Seawater: Its Composition, Properties and Behavior*, 2nd ed. Oxford, U.K.: Butterworth-Heinemann, 1995, ch. 2, pp. 14–28.

[5] A. Colling, *Ocean Circulation*, 2nd ed. Oxford, U.K.: Butterworth-Heinemann, 2001, ch. 4, pp. 133–137.

[6] P. K. Kundu, *Fluid Mechanics*. London, U.K.: Academic, 1990, ch. 13, pp. 489–496.

[7] S. R. Ramp, J. D. Paduan, I. Shulman, J. Kindle, F. L. Bahr, and F. Chavez, "Observations of upwelling and relaxation events in the northern Monterey Bay during August 2000," *J. Geophys. Res.*, vol. 110, 2005, C07013.

[8] W. M. Graham and J. L. Largier, "Upwelling shadows as nearshore retention sites: The example of northern Monterey Bay," *Continental Shelf Res.*, vol. 17, pp. 509–532, 1997.

[9] J. P. Ryan, D. Greenfield, R. M. III, C. Preston, B. Roman, S. Jensen, D. Pargett, J. Birch, C. Mikulski, G. Doucette, and C. Scholin, "Harmful phytoplankton ecology studies using an autonomous molecular analytical and ocean observing network," *Limnol. Oceanogr.*, vol. 56, no. 4, pp. 1255–1272, 2011.

[10] J. B. J. Harvey, J. P. Ryan, R. M. III, C. M. Preston, N. Alvarado, C. A. Scholin, and R. C. Vrijenhoek, "Robotic sampling, in situ monitoring and molecular detection of marine zooplankton," *J. Exp. Mar. Biol. Ecol.*, vol. 413, pp. 60–70, Feb. 2012.

[11] H. Schmidt, J. G. Bellingham, M. Johnson, D. Herold, D. M. Farmer, and R. Pawlowicz, "Real-time frontal mapping with AUVs in a coastal environment," in *Proc. MTS/IEEE OCEANS Conf.*, Sep. 1996, pp. 1094–1098.

[12] J. G. Bellingham, "New oceanographic uses of autonomous underwater vehicles," *Mar. Technol. Soc. J.*, vol. 31, no. 3, pp. 34–47, 1997, Fall.

[13] J. G. Bellingham, B. A. Moran, Y. Zhang, J. S. Willcox, N. Cruz, R. Grieve, J. J. Leonard, and J. W. Bales, "Haro Strait Experiment 1996 MIT Sea Grant Component," MIT Sea Grant AUV Lab, Cambridge, MA, Tech. Rep., 1997.

[14] Y. Zhang and J. S. Willcox, "Current velocity mapping using an AUV-borne acoustic doppler current profiler," in *Proc. 10th Int. Symp. Unmanned Untethered Submersible Technol.*, Durham, NH, Sep. 1997, pp. 31–40.

[15] A. R. Robinson, H. G. Arango, A. Warn-Varnas, W. G. Leslie, A. J. Miller, P. J. Haley, and C. J. Lozano, "Real-time regional forecasting," in *Modern Approaches to Data Assimilation in Ocean Modeling*, ser. Oceanography, P. Mallanotte-Rizzoli, Ed. Amsterdam, The Netherlands: Elsevier Science, 1996, pp. 377–412.

[16] H. C. Woithe and U. Kremer, "A programming architecture for smart autonomous underwater vehicles," in *Proc. IEEE Int. Conf. Intell. Robots Syst.*, St. Louis, MO, Oct. 2009, pp. 4433–4438.

[17] D. Wang, P. F. J. Lermusiaux, P. J. Haley, D. Eickstedt, W. G. Leslie, and H. Schmidt, "Acoustically focused adaptive sampling and on-board routing for marine rapid environmental assessment," *J. Mar. Syst.*, vol. 78, pp. S393–S407, 2009.

[18] F. Cazenave, Y. Zhang, E. McPhee-Shaw, J. G. Bellingham, and T. Stanton, "High-resolution surveys of internal tidal waves in Monterey Bay, California, using an autonomous underwater vehicle," *Limnol. Oceanogr., Methods*, vol. 9, pp. 571–581, 2011.

[19] N. Cruz and A. C. Matos, "Reactive AUV motion for thermocline tracking," in *Proc. IEEE OCEANS Conf.*, Sydney, Australia, May 2010, DOI: 10.1109/OCEANSSYD.2010.5603883.

[20] N. Cruz and A. C. Matos, "Adaptive sampling of thermoclines with autonomous underwater vehicles," in *Proc. MTS/IEEE OCEANS Conf.*, Seattle, WA, Sep. 2010, DOI: 10.1109/OCEANS.2010.5663903.

[21] S. Petillo, A. Balasuriya, and H. Schmidt, "Autonomous adaptive environmental assessment and feature tracking via autonomous underwater vehicles," in *Proc. IEEE OCEANS Conf.*, Sydney, Australia, May 2010, DOI: 10.1109/OCEANSSYD.2010.5603513.

[22] Y. Zhang, J. G. Bellingham, M. Godin, J. P. Ryan, R. S. McEwen, B. Kieft, B. Hobson, and T. Hoover, "Thermocline tracking based on peak-gradient detection by an autonomous underwater vehicle," in *Proc. MTS/IEEE OCEANS Conf.*, Seattle, WA, Sep. 2010, DOI: 10.1109/OCEANS.2010.5664545.

[23] D. P. Eickstedt, M. R. Benjamin, D. Wang, and H. Schmidt, "Behavior based adaptive control for autonomous oceanographic sampling," in *Proc. Int. Conf. Robot. Autom.*, Rome, Italy, Apr. 2007, pp. 4245–4250.

[24] E. Fiorelli, N. E. Leonard, P. Bhatta, D. A. Paley, R. Bachmayer, and D. M. Fratantoni, "Multi-AUV control and adaptive sampling in Monterey Bay," *IEEE J. Ocean. Eng.*, vol. 31, no. 4, pp. 935–948, Oct. 2006.

[25] K. Rajan, F. Py, C. McGann, J. Ryan, T. O'Reilly, T. Maughan, and B. Roman, "Onboard adaptive control of AUVs using automated planning and execution," in *Proc. 16th Int. Symp. Unmanned Untethered Submersible Technol.*, Durham, NH, Aug. 2009, pp. 1–13.

[26] Y. Zhang, J. P. Ryan, J. G. Bellingham, J. Harvey, R. S. McEwen, F. Chavez, and C. Scholin, "Classification of water masses and targeted sampling of ocean plankton populations by an autonomous underwater vehicle," presented at the AGU Fall Meeting, San Francisco, CA, Dec. 2011, Abstract OS21A-1609.

[27] Y. Zhang, M. Godin, J. G. Bellingham, and J. P. Ryan, "Ocean front detection and tracking by an autonomous underwater vehicle," in *Proc. MTS/IEEE OCEANS Conf.*, Kona, HI, Sep. 2011.

[28] J. G. Bellingham, Y. Zhang, J. E. Kerwin, J. Erikson, B. Hobson, B. Kieft, M. Godin, R. McEwen, T. Hoover, J. Paul, A. Hamilton, J. Franklin, and A. Banka, "Efficient propulsion for the Tethys long-range autonomous underwater vehicle," in *Proc. IEEE Autonomous Underwater Veh.*, Monterey, CA, Sept. 2010, DOI: 10.1109/AUV.2010.5779645.

[29] J. G. Bellingham, B. Hobson, M. A. Godin, B. Kieft, J. Erikson, R. McEwen, C. Kecy, Y. Zhang, T. Hoover, and E. Mellinger, "A small, long-range AUV with flexible speed and payload," presented at the Ocean Sci. Meeting, Portland, OR, Feb. 2010, Abstract MT15A- 14.

Yanwu Zhang (S'95–M'00–SM'05) was born in 1969 in Shaanxi Province, China. He received the B.S. degree in electrical engineering and the M.S. degree in underwater acoustics engineering from Northwestern Polytechnic University, Xi'an, China, in 1989 and 1991, respectively, the M.S. degree in electrical engineering and computer science from the Massachusetts Institute of Technology (MIT), Cambridge, in 1998, and the Ph.D. degree in oceanographic engineering from the MIT/Woods Hole Oceanographic Institution (WHOI) Joint Program, Cambridge/Woods Hole, MA, in June 2000.

From 2000 to 2004, he was a Systems Engineer working on medical image processing at the General Electric Company (GE) Research and Development Center, Niskayuna, NY, and then a Senior Digital Signal Processing (DSP) Engineer at Aware Inc., Bedford, MA, working on digital communications. Since December 2004, he has been with the Monterey Bay Aquarium Research Institute, Moss Landing, CA, as a Senior Research Specialist. He works on developing and field-testing adaptive sampling algorithms for autonomous underwater vehicles (AUVs) and applying them in ocean experiments, designing sampling strategy for ocean observatories comprising AUVs and moorings, and developing the long-range AUV Tethys. His current research interests are mainly in

spatio–temporal real-time signal processing and its applications to AUV's sampling of oceanographic processes.

Dr. Zhang was a finalist for the MIT *Technology Review Magazine*'s 100 young innovators (TR100) in 1999. He has participated in 12 field experiments running the Odyssey IIB, Dorado, and Tethys AUVs. He has served as a reviewer for the IEEE JOURNAL OF OCEANIC ENGINEERING and eight other academic journals, as well as for the National Science Foundation (NSF) and National Oceanic and Atmospheric Administration (NOAA) proposals. He was an invited session chair at the American Geophysical Union (AGU) 2007 Fall Meeting and the 2010 MTS/IEEE Oceans Conference. He is a member of the American Geophysical Union (AGU) and Sigma Xi.

Michael A. Godin was born in Westfield, MA, in 1968. He received the B.S. degree in mechanical engineering from the Worcester Polytechnic Institute (WPI), Worcester, MA, in 1991 and the M.S. degree in nuclear engineering from the Massachusetts Institute of Technology (MIT), Cambridge, in 1994.

He worked at the U.S. Department of Energy headquarters, Washington DC, from 1991 to 1998, first on robotic handing of spent nuclear fuel, and later on program management of nuclear waste cleanup research. From 1998 to 2003, he worked at Hydro-Optics, Biology, and Instrumentation Labs (HOBI Labs), Watsonville, CA, on the hardware design, software design, and manufacturing of underwater optical sensors and submersible data loggers. Since 2004, he has worked at the Monterey Bay Aquarium Research Institute (MBARI), Moss Landing, CA, where he has developed collaboration systems for geographically distributed groups of researchers, tools for spatio–temporal data exploration, and on a new software architecture for implementing state configured layered control on the Tethys AUV.

Mr. Godin chaired sessions at the 2007 and 2010 MTS/IEEE OCEANS Conferences, and serves on the SciDB Science Advisory Board.

James G. Bellingham (M'10) received the B.S./M.S. degrees in physics and the Ph.D. degree in physics from the Massachusetts Institute of Technology (MIT), Cambridge, in 1984 and 1988, respectively.

He is the Chief Technologist at the Monterey Bay Aquarium Research Institute (MBARI), Moss Landing, CA. His personal research activity revolves around the development and use of autonomous underwater vehicles (AUVs). He leads the Autonomous Ocean Sampling Network (AOSN) program at MBARI, which uses fleets of autonomous vehicles to adaptively observe dynamic oceanographic processes. He has spent considerable time at sea, leading over 20 AUV expeditions in environments ranging from the waters off Antarctica to the central Arctic. Before joining MBARI, he was at MIT, where he founded the Autonomous Underwater Vehicle Laboratory and ran it from 1988 to 2000. In 1997, he cofounded Bluefin Robotics Corporation, a leading manufacturer of AUVs.

Dr. Bellingham received the Lockheed Martin Award for Ocean Science and Engineering from the Marine Technology Society. He serves on a number of advisory boards and councils, including the Naval Research Advisory Committee and the Strategic Advisory Group for Battelle's National Security Division.

John P. Ryan was born in Lafayette, IN, in 1965. He received the B.S. degree in biology from the University of Massachusetts, Boston, in 1988 and the M.S. and Ph.D. degrees in biological oceanography from the University of Rhode Island, Narragensett, in 1993 and 1998, respectively.

He began a postdoctoral research position at the Monterey Bay Aquarium Research Institute (MBARI), Moss Landing, CA, in fall 1998, transitioned to MBARI Scientist in 2001, and is now Senior Research Specialist. His research integrates multidisciplinary observations from satellites, aircraft, ships, moorings, autonomous underwater vehicles (AUVs), and towed undulating vehicles to study ocean processes. In this research, he works extensively with engineers to advance AUV capabilities for marine science.

Dr. Ryan was awarded a fellowship by the Office of Naval Research in support of his M.S., and a NASA New Investigator Research grant in support of his postdoctoral research.